IEEE Sensors Letters Volume 2(3) (2017) Article #

Optical sensor

LMR-based Optical Sensor for Ethylene Detection at Visible and Mid-Infrared Regions

Elieser E. Gallego Martínez[1,2], Mikel Hualde Otamendi.[1], Carlos Ruiz Zamarreño[1,3]*, and Ignacio R. Matías[1,3]**

[1] *Dept. of Electrical, Electronic and Communication Engineering, Public University of Navarra, Pamplona, 31006, Spain*
[2] *Dept. of Telecommunications and Electronics, University of Pinar del Río, Pinar del Río, 20100, Cuba*
[3] *Institute of Smart Cities, Jerónimo de Ayanz Building, Pamplona, 31006, Spain*
** Senior Member, IEEE*
*** Fellow, IEEE*

Received 10 Jun 2023, revised 25 Jul 2023, accepted 30 Jul 2023, published 5 Sep 2023, current version 5 Sep 2023. (Dates will be inserted by IEEE; "published" is the date the accepted preprint is posted on IEEE Xplore®; "current version" is the date the typeset version is posted on Xplore®).

Abstract—Ethylene monitoring has long been a method of controlling the ripening of climacteric fruits. But it turns out that this gas is an important biomarker in biomedical applications. This work presents an optical gas sensor based on the lossy mode resonance (LMR) effect for ethylene detection in planar waveguide configuration. Two different approaches have been explored: one in the visible (VIS) spectral region and the second one in the mid infrared (MIR) region. Optical resonances have been achieved, in all cases, by means of sputtered tin oxide thin films. Response and recovery times were 54 and 246 s respectively for the sensor with the resonance in the VIS region while the device operating in the MIR obtained response and recovery times of 19 s and 47 s respectively. The sensitivity during ethylene detection varied from 93.8 pm/ppm to 187.5 pm/ppm with the devices working in the VIS and MIR regions, respectively. According to the calibration curve, devices shown an ethylene limit of detection (LOD) of 4.0058 ppm and 0.6532 ppm in the VIS and MIR spectral regions respectively, which finds applications in climacteric fruit ripening assessment as well as hemodialysis control. Cross sensitivity with humidity was also characterized for both devices.

Index Terms—Optical Sensor, Gas Sensor, Lossy Mode Resonance, Ethylene Sensor.

I. INTRODUCTION

Environmental pollution monitoring due to hazardous gases emission is a constant concern nowadays for health and safety among other reasons. The need to control precisely the concentrations of different gaseous species in industries as well as biomedical applications is increasing considerably the demand and the research efforts on highly sensitive and reliable gas sensors [1].

Particularly, ethylene is a traditional indicator used for fruits ripening assessment [2] but not exclusively. Ethylene also finds applications as biomarker for lipid peroxidation and oxidative stress in the exhaled breath of elderly patients with renal failure immediately after hemodialysis (HD) [3]. In particular, a patient average increase from 0.15 to 0.8 ppm of ethylene in breath was found after HD [3]. This gas, also known as ethene, is an organic chemical compound formed by two carbon atoms linked by a double bond. Ethylene is very well known by its effect upon plant growth and development, and it is cataloged as a regulator of organ senescence, stress responses, and pathogen responses [4].

LMR-based sensors have been successfully proven in the past as useful sensing tools using optical fiber configuration [5] and recently also in a planar waveguide configuration [6]. A metallic oxide thin-film is typically used for LMR generation, such as tin oxide that fulfills all the necessary conditions for the LMR to be generated. Its operating principle is based on resonance displacements produced by changes in the effective refractive index of the external medium [7]. Regarding gas sensing applications, optical fiber LMR-based devices have demonstrated to be suitable for humidity [8, 9] and hydrogen sulfide [10] detection. LMR-based devices have also been successfully used in planar waveguide configuration for the detection of acetone, ammonia and ethanol in the visible spectral region [11], and for 1-butanol detection in the mid infrared region [12].

SnO_2 is the most widely used material as sensitive to ethylene for sensing purpose [13-23], but not combined to LMR effect till now.

This work presents the utilization of LMR-based devices in planar waveguide configuration for ethylene detection in the visible and mid infrared regions by means of SnO_2 sputtered thin film.

II. SENSOR DESIGN AND EXPERIMENTAL SETUP

A. Device Fabrication

Two devices were fabricated and characterized for ethylene detection, both in planar waveguide configuration. The first one (sensor A, Fig.1a), using a 18 x 18 mm and 130 µm thick standard borosilicate glass coverslip as waveguide, and the other one (sensor B, Fig.1b) using a 10 x 10 mm and 500 µm thick CaF_2 (from UQG Optics). Tin oxide thin-films were deposited onto the planar waveguides by means of DC-sputtering using a Benchtop High-Vacuum Magnetron Sputtering System purchased from MOORFIELD and a tin oxide target. The fabrication conditions were:

Corresponding author: E. E. G. M. Author (elieser.gallego@unavarra.es).

Digital Object Identifier: 10.1109/LSEN.XXXX.XXXXXXX (inserted by IEEE).

120 mA current, 1.2 × 10-2 mBar vacuum pressure and a distance of 10 cm between the substrates and the target.

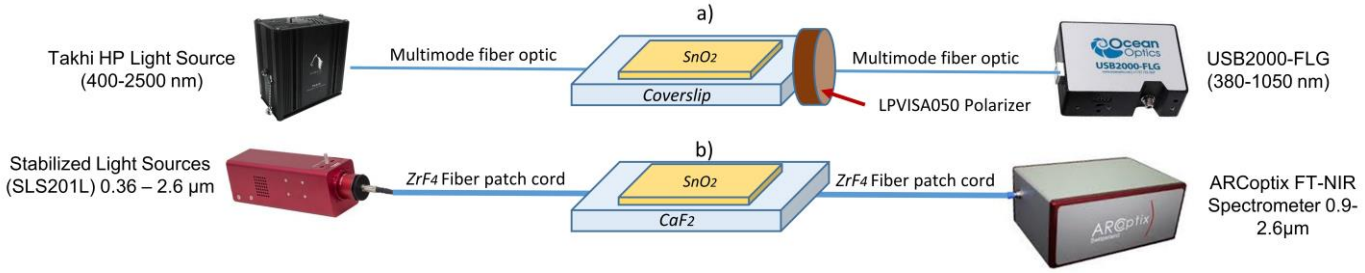

Fig. 1. Experimental setup used for sensor A (a) and sensor B (b).

B. Experimental measuring setup

Sensor A experimental setup (Fig.1a) consisted of a typical transmission setup in the visible region comprising a Takhi-HP light source (from Pyroistech Inc.) coupled to a multimode optical fiber (200/225 µm core/cladding diameter purchased from Thorlabs Inc.), an USB2000FLG spectrometer (Ocean Optics Inc.), and a LPVISA050 polarizer (obtained from Thorlabs Inc.). Sensor B setup in the mid infrared region consisted of a stabilized light source, SLS201L (from Thorlabs Inc.) coupled to a 500 µm core diameter fluorinated zirconium (ZrF_4) optical fiber patch cord (MZ41L1, purchased from Thorlabs Inc.) with a working range up to 4.5 µm and an ARCoptix (Arcoptix Switzerland) FTIR spectrometer.

Gas measurements were performed with the sensors in a sealed chamber with gas inlet and exhaust. Ethylene gas cylinder with a concentration of 200 ppm (purchased from Nippon Gases) was used for ethylene sensitivity measurements. To achieve stable measurement conditions, a nitrogen (N_2) carrier gas was used, so that the total flow rate was fixed at 300 mL/min during the experiments. Table 1 shows the gas flow combinations used for N_2 and ethylene during the experiments and the obtained concentrations of ethylene for each case.

Table 1. N_2 and ethylene gas flow combinations and ethylene concentrations.

Condition	N_2 flow [mL/min]	Ethylene flow [mL/min]	[Ethylene] [ppm]
1	300	0	0
2	275	25	16
3	250	50	32
4	225	75	*50*
5	200	100	*66*

In this work, the lowest ethylene flow value (25 mL/min) was chosen in order to guarantee the proper operation of the gas flow controller (from Bronkhorst, NL-7261 AK Ruurlo, Netherlands), which was not qualified for lower values. Therefore, the lowest ethylene concentration used in our experiments (16ppm) was defined based on measurement conditions and not on sensor performance.

Water vapor cross sensitivity was also tested in both A and B devices. In this case, deionized ultrapure water was pressurized and vaporized with a controlled evaporated mixer (CEM, from Bronkhorst, NL-7261 AK Ruurlo, Netherlands). Flow control of the CEM is expressed in mg/h. Table 2 shows the water vapor mass flow that is combined in each case with a constant nitrogen carrier flow of 300 mL/min in order to provide a fixed water vapor concentration and relative humidity inside the sealed chamber.

Table 2. Water vapor concentrations and equivalent relative humidity for 300 mL/min nitrogen carrier gas.

Condition	Water vapor mass flow [mg/h]	Concentration [ppm]	RH (%)
1	0	0	0
2	50	3442	12
3	100	6860	24
4	150	10255	36
5	200	13627	48

Response and recovery times for both sensors were calculated as the LMR wavelength shift time from 10 % to 90% and vice versa.

For both devices, first order resonance was used as reference for measurements, at 560 nm for sensor A and at 2320 nm for sensor B.

III. RESULTS AND DISCUSSION

Fig. 2.a) shows the response of sensor A to concentrations of ethylene in the range from 16 to 66 ppm. Figure 2.b) shows the response of sensor A to relative humidity in the range from 12 to 48%.

The response and recovery times of this sensor A to ethylene were 54 s and 246 s respectively, achieving a sensitivity of 93.8 pm/ppm. Humidity response and recovery times of sensor A were 54 s and 48 s respectively, achieving a sensitivity of 1.5 pm/ppm (or 417 pm/%RH).

Previous experiments were also repeated with sensor B in order to compare the performance with sensor A. Figure 3 shows the results of sensor B when it was exposed to the same ethylene concentrations and the same relative humidity levels as sensor A. The response and recovery times of sensor B for ethylene were 19 s and 47 s respectively. In the case of relative humidity, the response and recovery times of sensor B were 34 s and 63 s respectively. The sensitivity of sensor B was 187.5 pm/ppm and 5.2 pm/ppm (or 1.5 nm/%RH) for ethylene and relative humidity respectively.

Fig. 4 calibration curves show the wavelength shift of the optical resonances of sensors A and B for different ethylene concentrations (Fig. 4a) and different relative humidity levels (Fig. 4b). Linearity factors (R^2) obtained for sensor A were 0.9427 and 0.9660 for ethylene and humidity respectively, while sensor B linearity factors were 0.9988 and 1 for ethylene and humidity respectively. Error bars in Figure 4 represent the deviation of the measurements from the averaged data points represented in the graph. According to the statistical properties obtained from the measured data of sensors A and B during ethylene detection, the LOD is 4.0058 ppm and 0.6532 ppm for sensors A and B respectively. These parameters were calculated using equation (1), were S_{dv} is the standard deviation, and

∂ is the slope of the calibration curve [24].

$$LOD = 3.3 * \frac{S_{dv}}{\partial} \quad (1)$$

Both sensors have shown good repeatability as it can be observed from the three repetitions at the beginning of the measurements in Figures 2 and 3. Particularly, sensor B revealed a higher sensitivity, faster response and recovery times and a higher linearity compared to sensor A (see Table 3), this reveals the enhanced performance of the device operating in the MIR range. On the other hand, the performance of sensor A could be also useful in specific applications where the high cost of MIR instrumentation could be a barrier and there is no demand for high sensitivity or fast response, such as climacteric fruit ripening assessment. Table 3 shows a brief summary of the parameters of both sensors, A and B, in order to facilitate their comparison.

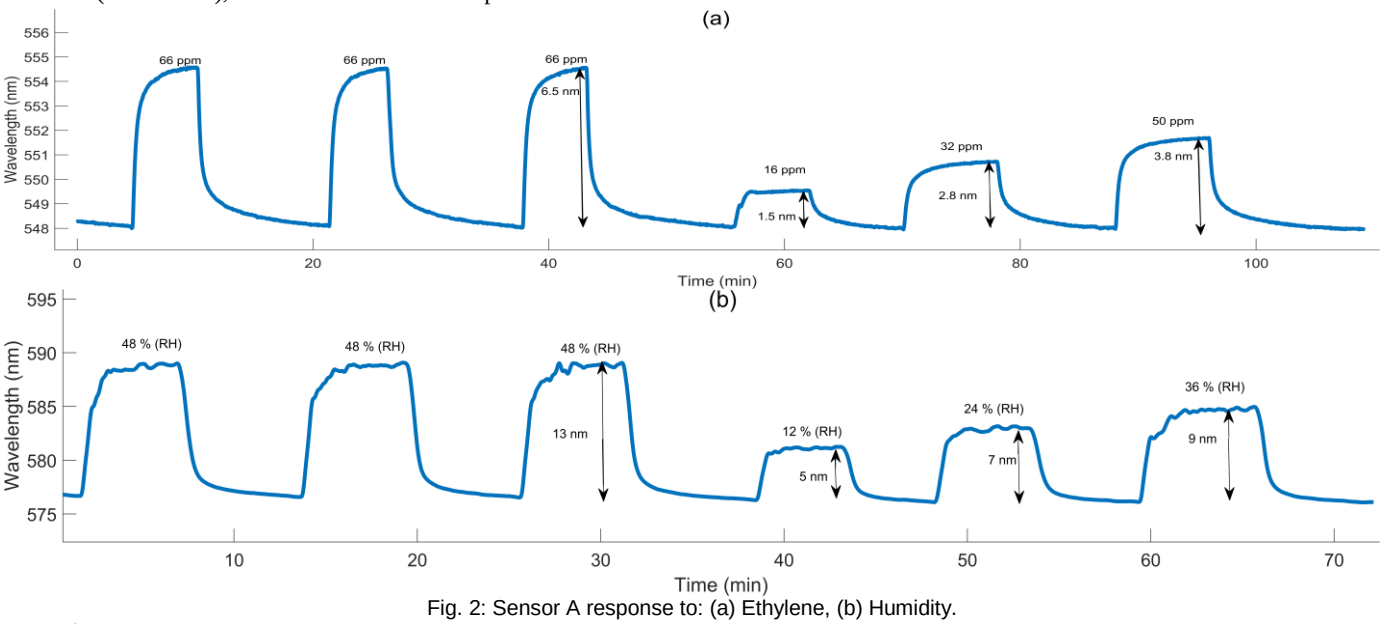

Fig. 2: Sensor A response to: (a) Ethylene, (b) Humidity.

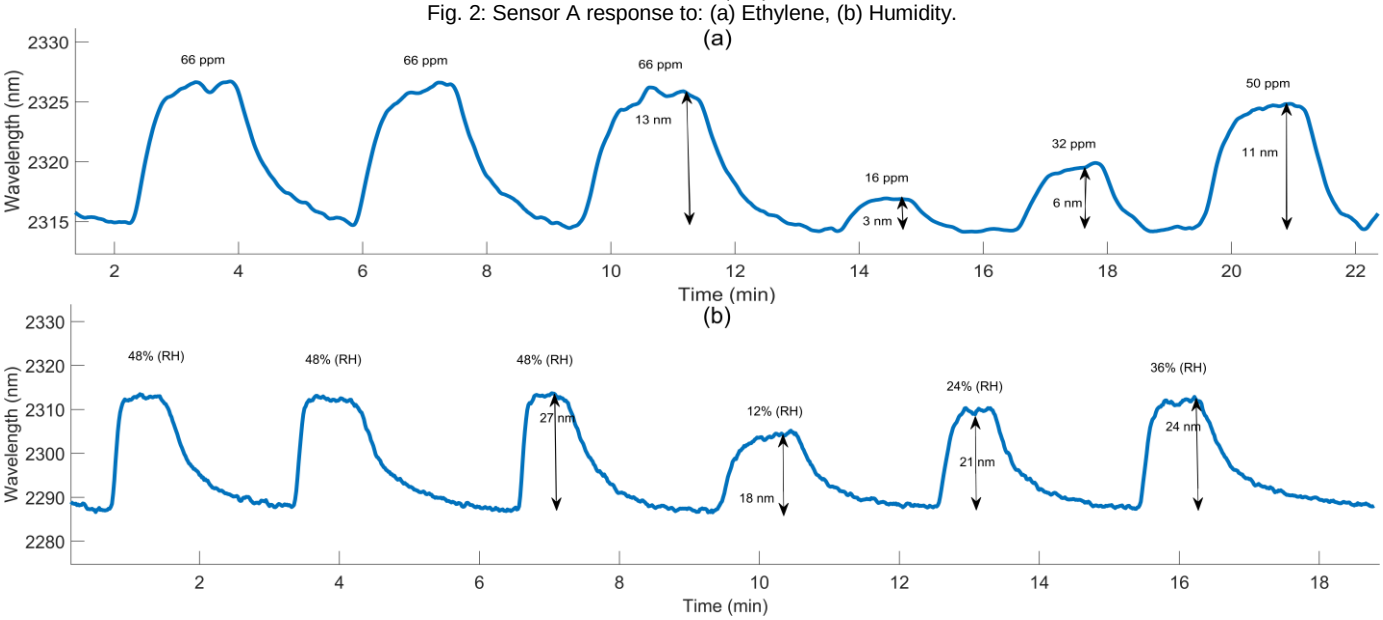

Fig. 3. Sensor B response to: (a) Ethylene, (b) Humidity.

Table 3. Sensors A and B performance.

	Gas Target	A	B
Response time [s]	Ethylene	54	19
	Humidity	53	34
Recovery time [s]	Ethylene	246	47
	Humidity	48	63
Sensitivity [pm/ppm]	Ethylene	93.8	187.5
	Humidity	1.5	5.2

IV. CONCLUSIONS

As an innovation of this study, LMR-based planar waveguide devices operating in the visible and mid infrared regions were successfully fabricated by means of tin oxide thin-films and tested for ethylene and relative humidity detection. A comparative study was also performed highlighting the advantages and disadvantages of each device.

The new findings confirm the feasibility of very simple and very low-cost planar waveguide configuration in the fabrication of optical

sensors based on LMR effect for gas detection and it is the first approach of LMR-based devices for ethylene detection. It is also important to remark that this work opens the door to the utilization of LMR-based devices for gas detection in biomedical applications. At the same time, this result represents an improvement compared to many other proposals [13-23] that use other materials and compounds or even the same tin oxide we used in this work.

In the case of sensor B, its LOD makes it feasible for biomedical applications where ethylene is used as biomarker for lipid peroxidation and oxidative stress in the exhaled breath of elderly patients with renal failure immediately after HD, given that its LOD is lower than 0.8 ppm (0.6532 ppm).

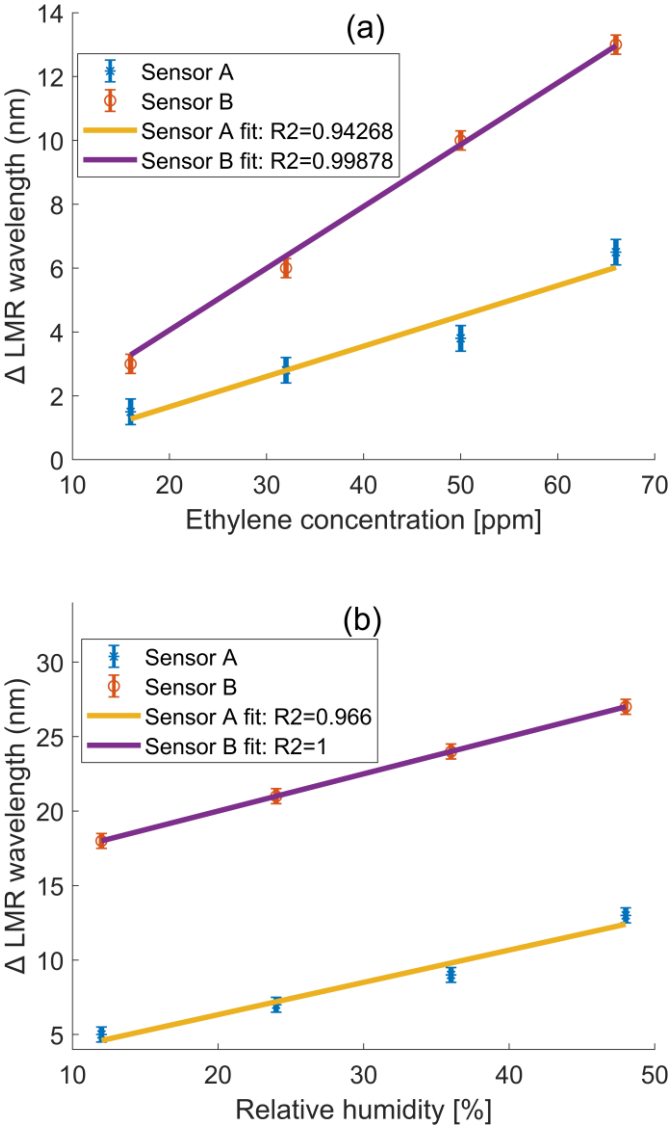

Figure 4: LMR shift for sensors A and B: (a) Ethylene, (b) Relative Humidity.

ACKNOWLEDGMENTS

This work was supported by Agencia Estatal de Investigación (PID2019-106231RB-I00), Institute Smart Cities and Public University of Navarra Ph.D. Student grants.

REFERENCES

[1] Oh, E. H., Song, H. S., & Park, T. H. (2011). Recent advances in electronic and bioelectronic noses and their biomedical applications. Enzyme and microbial technology, 48(6-7), 427-437.
[2] Janssen, S., Schmitt, K., Blanke, M., Bauersfeld, M. L., Wöllenstein, J., & Lang, W. (2014). Ethylene detection in fruit supply chains. Philosophical Transactions of the Royal Society A: Mathematical, Physical and Engineering Sciences, 372(2017), 20130311.
[3] Popa, C., Patachia, M., Banita, S., Matei, C., Bratu, A. M., & Dumitras, D. C. (2013). The level of ethylene biomarker in the renal failure of elderly patients analyzed by photoacoustic spectroscopy. Laser Physics, 23(12), 125701.
[4] Schaller, G. E., & Kieber, J. J. (2002). Ethylene. The Arabidopsis book/American Society of Plant Biologists, 1.
[5] Del Villar, I., Zamarreño, C. R., Hernaez, M., Arregui, F. J., & Matias, I. R. (2009). Lossy mode resonance generation with indium-tin-oxide-coated optical fibers for sensing applications. Journal of Lightwave Technology, 28(1), 111-117.
[6] Fuentes, O., Corres, J. M., Matias, I. R., & Del Villar, I. (2019). Generation of lossy mode resonances in planar waveguides toward development of humidity sensors. Journal of Lightwave Technology, 37(10), 2300-2306.
[7] Del Villar, I., Hernaez, M., Zamarreño, C. R., Sánchez, P., Fernández-Valdivielso, C., Arregui, F. J., & Matias, I. R. (2012). Design rules for lossy mode resonance based sensors. Applied optics, 51(19), 4298-4307.
[8] Zamarreño, C. R., Hernaez, M., Del Villar, I., Matias, I. R., & Arregui, F. J. (2010). Tunable humidity sensor based on ITO-coated optical fiber. Sensors and Actuators B: Chemical, 146(1), 414-417.
[9] Zamarreño, C. R., Hernaez, M., Sanchez, P., Del Villar, I., Matias, I. R., & Arregui, F. J. (2011). Optical fiber humidity sensor based on lossy mode resonances supported by TiO2/PSS coatings. Procedia Engineering, 25, 1385-1388.
[10] Usha, S. P., Mishra, S. K., & Gupta, B. D. (2015). Fiber optic hydrogen sulfide gas sensors utilizing ZnO thin film/ZnO nanoparticles: A comparison of surface plasmon resonance and lossy mode resonance. Sensors and Actuators B: Chemical, 218, 196-204.
[11] Vitoria, I., Gallego, E. E., Melendi-Espina, S., Hernaez, M., Ruiz Zamarreño, C., & Matías, I. R. (2023). Gas sensor based on lossy mode resonances by means of thin graphene oxide films fabricated onto planar coverslips. Sensors, 23(3), 1459.
[12] Martínez, E. G., Matias, I. R., Melendi-Espina, S., Hernaez, M., & Zamarreño, C. R. (2023). Lossy mode resonance based 1-butanol sensor in the mid-infrared region. Sensors and Actuators B: Chemical, 388, 133845.
[13] Esser, B., Schnorr, J. M., & Swager, T. M. (2012). Selective detection of ethylene gas using carbon nanotube-based devices: utility in determination of fruit ripeness. Angewandte Chemie International Edition, 51(23), 5752-5756.
[14] Pattananuwat, P., & Aht-Ong, D. (2010, October). Electrochemical synthesis of sensitive layer of polyaniline: effects of acid doping on ethylene gas sensing. In Materials Science Forum (Vol. 654, pp. 2285-2288). Trans Tech Publications Ltd.
[15] Kathirvelan, J., & Vijayaraghavan, R. (2014). Development of prototype laboratory setup for selective detection of ethylene based on multiwalled carbon nanotubes. Journal of Sensors, 2014.
[16] Pattananuwat, P., & Aht-Ong, D. (2013). In-situ electrochemical synthesis of novel sensitive layer of polyaniline/multiwall carbon nanotube/tin oxide hybrid materials for ethylene gas detection. Polymer-Plastics Technology and Engineering, 52(2), 189-194.
[17] Kathirvelan, J., Vijayaraghavan, R., & Thomas, A. (2017). Ethylene detection using TiO2–WO3 composite sensor for fruit ripening applications. Sensor Review, 37(2), 147-154.
[18] Nimittrakoolchai, O. U., & Supothina, S. (2008). High-yield precipitation synthesis of tungsten oxide platelet particle and its ethylene gas-sensing characteristic. Materials Chemistry and Physics, 112(1), 270-274.
[19] Wang, L. P., Jin, Z., Luo, T., Ding, Y., Liu, J. H., Wang, X. F., & Li, M. Q. (2019). The detection of ethylene using porous ZnO nanosheets: Utility in the determination of fruit ripeness. New Journal of Chemistry, 43(8), 3619-3624.
[8] Ivanov, P., Llobet, E., Vergara, A., Stankova, M., Vilanova, X., Hubalek, J., ... & Correig, X. (2005). Towards a micro-system for monitoring ethylene in warehouses. Sensors and Actuators B: Chemical, 111, 63-70.
[20] Jadsadapattarakul, D., Thanachayanont, C., Nukeaw, J., & Sooknoi, T. (2010). Improved selectivity, response time and recovery time by [0 1 0] highly preferred-orientation silicalite-1 layer coated on SnO2 thin film sensor for selective ethylene gas detection. Sensors and Actuators B: Chemical, 144(1), 73-80.
[21] Ahn, H., Noh, J. H., Kim, S. B., Overfelt, R. A., Yoon, Y. S., & Kim, D. J. (2010). Effect of annealing and argon-to-oxygen ratio on sputtered SnO2 thin film sensor for ethylene gas detection. Materials Chemistry and Physics, 124(1), 563-568.
[22] Zhao, Q., Duan, Z., Yuan, Z., Li, X., Si, W., Liu, B., ... & Tai, H. (2020). High performance ethylene sensor based on palladium-loaded tin oxide: Application in fruit quality detection. Chinese Chemical Letters, 31(8), 2045-2049.
[23] Tolentino, M. A. K. P., Albano, D. R. B., & Sevilla III, F. B. (2018). Piezoelectric sensor for ethylene based on silver (I)/polymer composite. Sensors and Actuators B: Chemical, 254, 299-306.
[24] Shrivastava, A., & Gupta, V. B. (2011). Methods for the determination of limit of detection and limit of quantitation of the analytical methods. Chron. Young Sci, 2(1), 21-25.